Improved Photoelectrical Properties of MoS_2 Films after Laser Micromachining

Junpeng Lu,[†] Jia Hui Lu,[†] Hongwei Liu,[‡] Bo Liu,[§] Kim Xinhui Chan,[†] Jiadan Lin,[†] Wei Chen,[†,∥] Kian Ping Loh,[§,∥] and Chorng Haur Sow[†,§,*]

[†]Department of Physics, National University of Singapore, 2 Science Drive 3, Singapore 117542, Singapore, [‡]Institute of Materials Research and Engineering, A*STAR (Agency for Science, Technology and Research), 3 Research Link, Singapore 117602, Singapore, [§]Graphene Research Centre, National University of Singapore, 6 Science Drive 2, Singapore 117546, Singapore, and [∥]Department of Chemistry, National University of Singapore, 3 Science Drive 3, Singapore 117543, Singapore

ABSTRACT Direct patterning of ultrathin MoS_2 films with well-defined structures and controllable thickness is appealing since the properties of MoS_2 sheets are sensitive to the number of layer and surface properties. In this work, we employed a facile, effective, and well-controlled technique to achieve micropatterning of MoS_2 films with a focused laser beam. We demonstrated that a direct focused laser beam irradiation was able to achieve localized modification and thinning of as-synthesized MoS_2 films. With a scanning laser beam, microdomains with well-defined structures and controllable thickness were created on the same film. We found that laser modification altered the photoelectrical property of the MoS_2 films, and subsequently, photodetectors with improved performance have been fabricated and demonstrated using laser modified films.

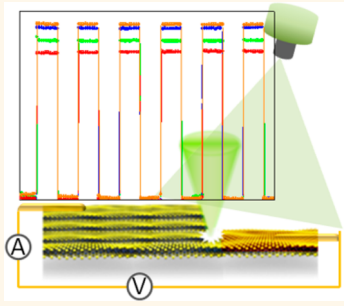

KEYWORDS: transition metal dichalcogenides · molybdenum disulfide · 2D materials · laser patterning · photodetector

As layered semiconducting analogues of graphene, transition metal dichalcogenides (TMDCs) have attracted great attention due to the intriguing existence of band gaps in their electronic structures, which is complementary to graphene-based electronic behaviors.[1−5] Among these TMDCs, MoS_2 is demonstrated as one of the most promising two-dimensional (2D) material due to its layer-dependent physical and chemical properties that arise in its monolayer form, such as the indirect to direct band gap transition,[6] photoluminescence (PL) transitions,[7] and alteration of Raman-active phonon modes.[8,9] Many studies have indeed demonstrated the promise of ultrathin MoS_2 in fields of low power switches,[10] field effect transistors,[3] optoelectronics[5] and spintronics.[11] Most of these devices were based on small size MoS_2 nanosheets fabricated by mechanical or chemical exfoliation of single layers from bulk crystals. Nevertheless, the applications were restricted by the limited capability in producing high quality and uniform large area MoS_2 films. Recently, considerable efforts have been attempted to achieve scalable synthesis of high quality large area MoS_2 monolayers to improve the possibility of device application.[8,12−16] Different strategies have been developed to produce MoS_2 monolayer and multilayers over a large area up to centimeters.[17,20] Simultaneously, postsynthesis procedures were explored to further control the layer number of the MoS_2 products. For example, Ni *et al.* reported a plasma technique for layer by layer thinning of mechanically exfoliated MoS_2[18] and Castellanos-Gomez *et al.* employed a focused laser beam to achieve on demand generation of single layer MoS_2.[19] Notably, the small size of the exfoliated products reported in these works could still restrict the device development. Until now, the facile technique which can postpattern, modify or decorate the large area MoS_2 films is absent. Once 2D TMDCs films with uniform thickness and large area coverage are fabricated, in light of the interest to create a functional device, it is worthwhile to develop techniques which can further create micropatterns with controlled functionalities on the MoS_2 films. These techniques should be able to directly pattern the MoS_2 films as well as to alter or modify the surface property or functionality of the thin films during the patterning process. Therefore, a simple, efficient, flexible, and

* Address correspondence to physowch@nus.edu.sg.

Received for review April 2, 2014 and accepted May 26, 2014.

Published online May 26, 2014
10.1021/nn501821z

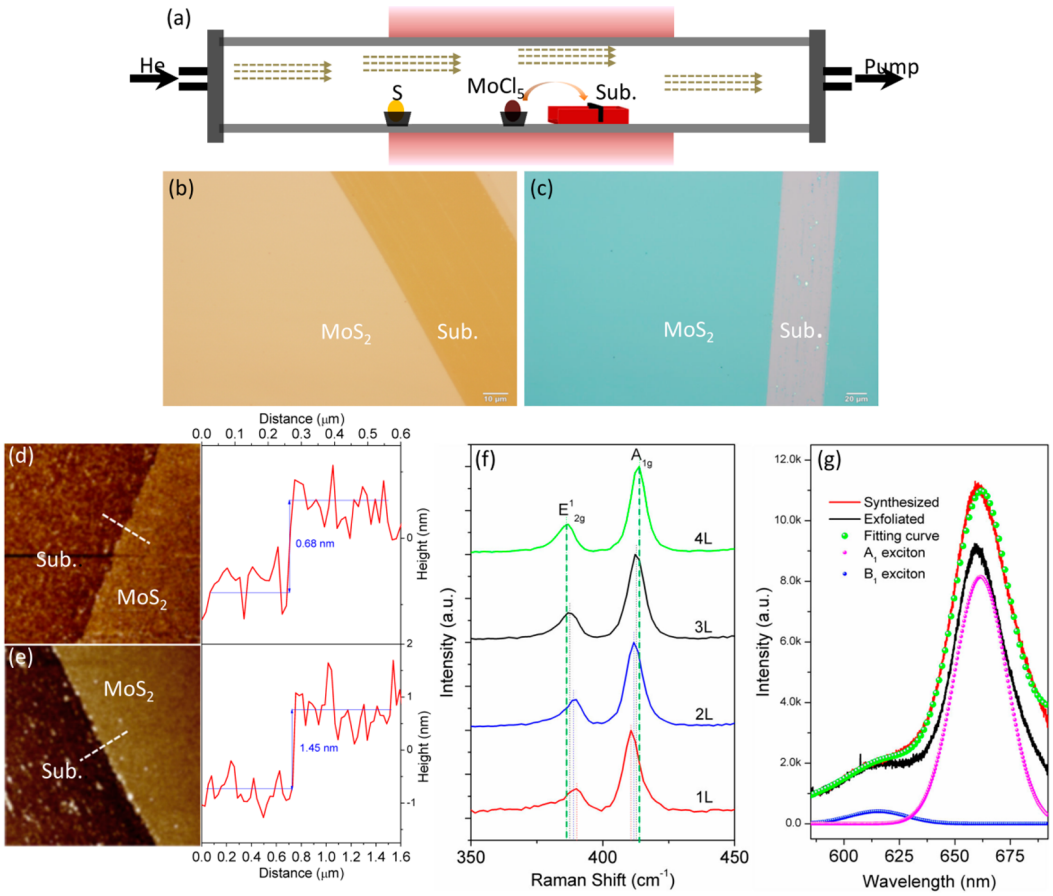

Figure 1. (a) Schematic diagram of large area MoS_2 films growth reactor. (b) Optical image of monolayer MoS_2 grown on sapphire substrate. (c) Optical image of bilayer MoS_2 grown on SiO_2/Si substrate. AFM images and height profiles of (d) monolayer and (e) bilayer MoS_2 films. (f) Raman spectra of MoS_2 films with different thicknesses. (g) PL spectra of as-synthesized monolayer MoS_2 (red curve) compared with exfoliated monolayer MoS_2 (black curve).

low cost multipurpose postprocessing technique is highly desirable. In this work, we built on the facile and effective focused laser thinning method[19] to controllably modify the property of large area multilayer MoS_2 films. Since property of the MoS_2 films depends on the number of layer, we can exploit this property and thus create different functional components within the same sample. First, by scanning the sample with respect to the focused laser beam, well-defined micropatterns were created on the multilayer films without using any predefined mask. Hence, this method reduced the risks of physical damage and chemical contamination to the sample. Second, a thinner layer was fabricated after laser modification. By controlling the laser thinning process, monolayer domain surrounded by multilayer film was achieved. With this approach, functional junctions composed of domains with different thicknesses and hence different band gaps were readily fabricated. In addition, the focused laser beam facilitated chemical modification of the thin films while it was thinned down. Finally, the focused laser pruning altered the photoelectrical property of the MoS_2 films. On the basis of this, a photodetector with improved performance was fabricated and demonstrated using laser modified MoS_2 films.

RESULTS AND DISCUSSIONS

In self-limiting growth approach, the thickness of the pristine MoS_2 films can be strongly affected by the amount of precursor, the total pressure and the deposition temperature.[17] To precisely control the thickness uniformity of the MoS_2 films, the substrate was vertically inserted into the slits of a custom-designed sample holder (Figure 1a). In doing so, the entire substrate was positioned in a zone with uniform temperature which was desirable for uniform growth. We have successfully grown MoS_2 films from monolayer to four-layers on various substrates (SiO_2/Si, quartz and sapphire) as shown in Figure S1. The optical images of monolayer and bilayer films grown on sapphire and SiO_2/Si substrates are shown in Figure 1, panels b and c, respectively. Note that we intentionally introduced scratches on the films to enhance the contrast of the images, from which the films were observed to be continuous and uniform over a large area. The thicknesses of these films were characterized by atomic force microscope (AFM). As shown in Figure 1d,e, the

thicknesses of two films were measured to be 0.68 and 1.45 nm, respectively.[3] This indicates the synthesized MoS_2 thin films were monolayer and bilayer, respectively. Raman spectroscopy has been demonstrated to be another effective tool to characterize the thickness of TMDCs thin films.[9,21] Figure 1f shows the Raman spectra collected from MoS_2 thin films with different thicknesses synthesized on SiO_2/Si substrates. Evidently, the Raman spectra of all film thickness show strong signals from both the in-plane E^1_{2g} and the out-of-plane A_{1g} vibration. The frequency spacing of these two peaks is measured to be 20.1 cm^{-1} for as-synthesized monolayer MoS_2. This value is slightly larger than that of exfoliated monolayer[9] and single crystalline as-grown monolayer[12,20] due to the crystalline imperfection of our sample.[8,17] It is obvious that the E^1_{2g} vibration red shifts, while the A_{1g} vibration blue shifts with increasing layer numbers. This phenomenon is consistent with that observed in exfoliated MoS_2 flakes.[9] Good optical property was expected from the monolayer film due to the direct band gap of MoS_2 in monolayer. Figure 1g red curve shows the PL spectrum of a monolayer MoS_2 synthesized in this work. After fitting the experimental data with Gaussian curves, the spectrum was found to be a combination of a major peak and a minor peak at around 660 and 617 nm, respectively. These peaks can be ascribed to the recombination of A_1 and B_1 excitons, suggesting the direct band gap photoluminescence from the K point.[7,22] As compared with exfoliated monolayer sample (black curve), the emission spectrum showed similar emission peak and suggested a comparable optical quality in the as-synthesized monolayer MoS_2 films. The PL spectrum with extended range was carried out and shown in Supporting Information Figure S2. Both the Raman and PL peaks are shown in the spectrum.

After the successful synthesis of the large area MoS_2 films with controllable layer numbers, we subjected the films to a postsynthesis treatment of focused laser beam destruction with the aim to create micropatterns on the substrate. However, instead of complete destruction of the films, we found that the focused laser beam could effectively and controllably thin the thickness of multilayer films and more importantly facilitate the creation of monolayer−multilayer domain at any selective position. In MoS_2 thin film, the band structure shows obvious layer-dependence, *i.e.*, the bulk indirect band gap of 1.3 eV increases to a direct band gap of 1.8 eV in single-layer form.[5,23] With this feasibility, we could carry out localized band gap engineering on a MoS_2 film and create domains with different band gap on the same sample.

The direct micropatterning and thinning of MoS_2 films was carried out through an optical microscope-focused laser beam setup. Figure 2a shows a schematic diagram of our experimental setup. In this setup, a diode laser (maximum power = 300 mW, λ = 532 nm) was employed. The emitted parallel laser beam was introduced into an optical microscope *via* two mirrors. Inside the microscope, the laser beam was directed toward the objective lens by a beam splitter. The laser beam was tightly focused onto the surface of a sample *via* an objective lens (magnification = 100×). The sample was mounted on an $X-Y$ stage (motorized stage MICOS) which was controlled by a computer. A CCD camera was used to capture the optical images. Hence we could monitor the process of laser thinning and examine the quality of the pattern directly. Besides modification of the sample in ambient condition, a vacuum chamber could be utilized to house the sample, as shown in Figure 2a. In doing so, the films can also be modified in vacuum condition (typical pressure in vacuum chamber is $\sim 10^{-2}$ mbar). When the laser beam was focused upon a MoS_2 film, the absorbed laser energy was rapidly converted to local heat. The intense heat raised the temperature of irradiated part and caused localized partial thinning of the films. When we controlled the sample stage movement in a programmable manner with respect to the focused laser beam, micropatterns were constructed on the MoS_2 films. Figure 2b shows the bright field optical image of a pattern created using this laser modification method, and Figure 2c shows the same pattern as observed under dark field. Figure 2d provides further illustrations on the appearance of the patterned samples when they were imaged by bright field light and dark field optical microscope, respectively. Remarkably, the laser modified region was not a region with destruction or removal of the MoS_2. Instead, a thinner layer would appear after laser modification. By careful control of the laser power and scanning speed, a thicker-layer to thinner-layer transition could be selectively achieved in the multilayer MoS_2 films, while leaving nonmodified region intact. Therefore, the monolayer domain surrounded by multilayer film was achieved by using high laser power (~85 mW) at a 50 μm/s scanning speed. Hence, with this approach, thin films with different functional components and also functional junctions based on the layer-dependent band gap engineering in MoS_2 could be readily fabricated. Moreover, the focused laser beam also facilitated chemical modification of the thin films while it was thinned down. As shown in Figure 2e, a monolayer MoS_2 domain surrounded by 4-layer film was created using this method. The Raman and PL spectra were carried out to verify the layer number of the pristine and laser modified regions. As shown in Figure 2f, the frequency difference between E^1_{2g} and A_{1g} modes obviously decreased after laser modification. The PL spectrum (Figure 2g) collected from the fabricated monolayer domain clearly showed the exciton peaks while the spectrum collected from the pristine region did not show any emission peak. Evidently, the appearance of

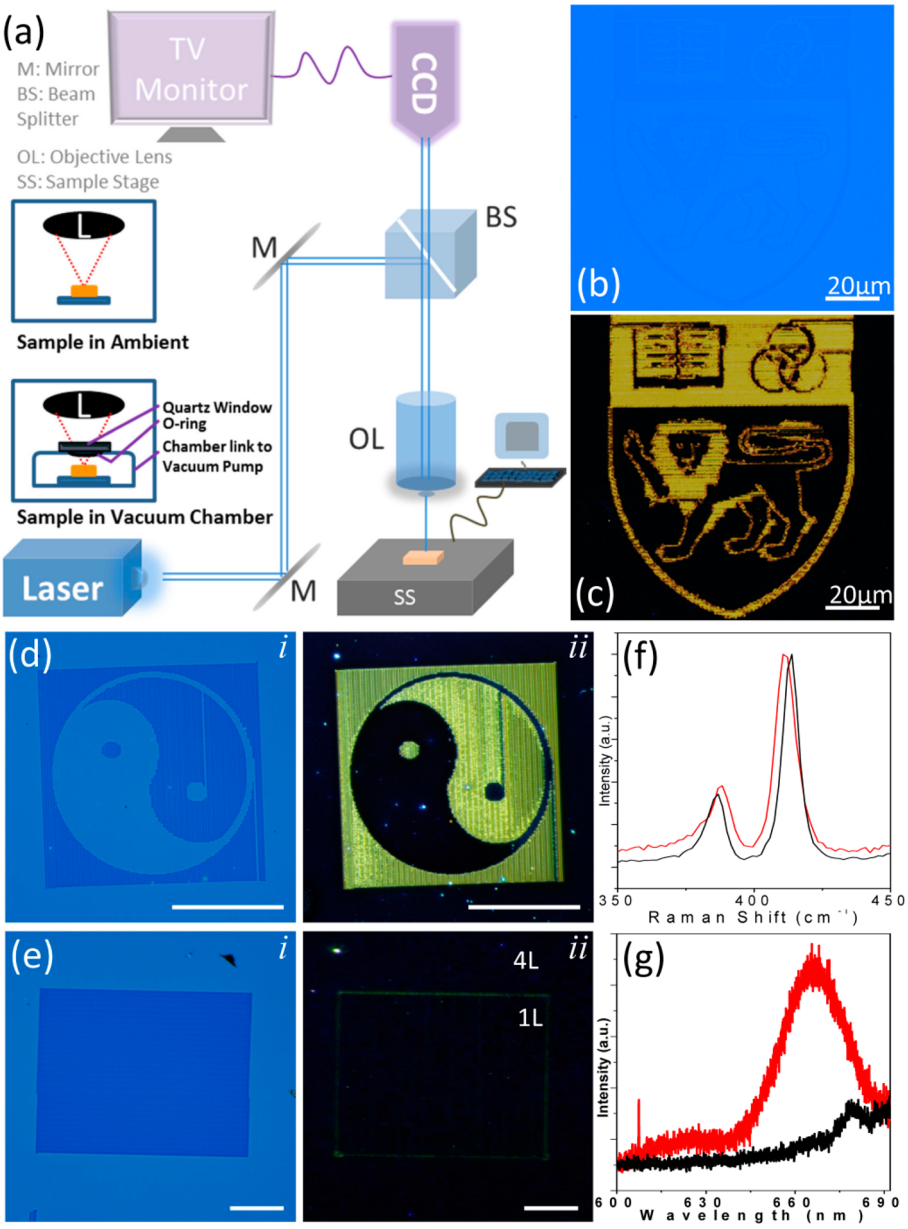

Figure 2. (a) Schematic of the focused laser beam setup for micropattering. (b) Optical image of a representative pattern. (c) Observed image of (b) under dark field. (d) A "Tai Chi" pattern observed under xenon light and dark field, respectively. (e) Optical images of a created monolayer square domain. (f) Raman and (g) PL spectra of pristine (black curve) and laser thinning (red curve) regions.

A_1 and B_1 exciton emission in the spectrum indicated the creation of direct band gap monolayer MoS_2. The thinning procedure was facilitated by the sublimation of the upper layers due to the heat generated by laser energy absorption. Similar to report by Castellanos-Gomez *et al.*,[19] the thermal energy could not be easily dissipated through the substrate due to the loose coupling between the MoS_2 layers since they are mediated by van der Waals forces. Besides the sublimation, partial oxidation of MoS_2 to MoO_3 is unavoidable during the laser modification process in ambient. The characterization of the modified products indicates the existence of MoO_3 which will be shown later in this report.

To illustrate the improved functionality of laser modified MoS_2 films, simple photoelectronic devices composed of MoS_2 film that bridged across two conducting electrodes were fabricated and characterized. Both pristine film and laser modified film were investigated in these experiments. The device fabrication was facilitated by a modified transfer procedure.[13] The assembly process is illustrated in Figure 3a. As shown by the last step, the MoS_2 films could be transferred to bare SiO_2/Si substrate for device fabrication or transferred onto substrate with prepatterned electrodes to directly assemble into devices. The top left corner of Figure 3a shows an optical image of a device made by covering two electrodes with MoS_2

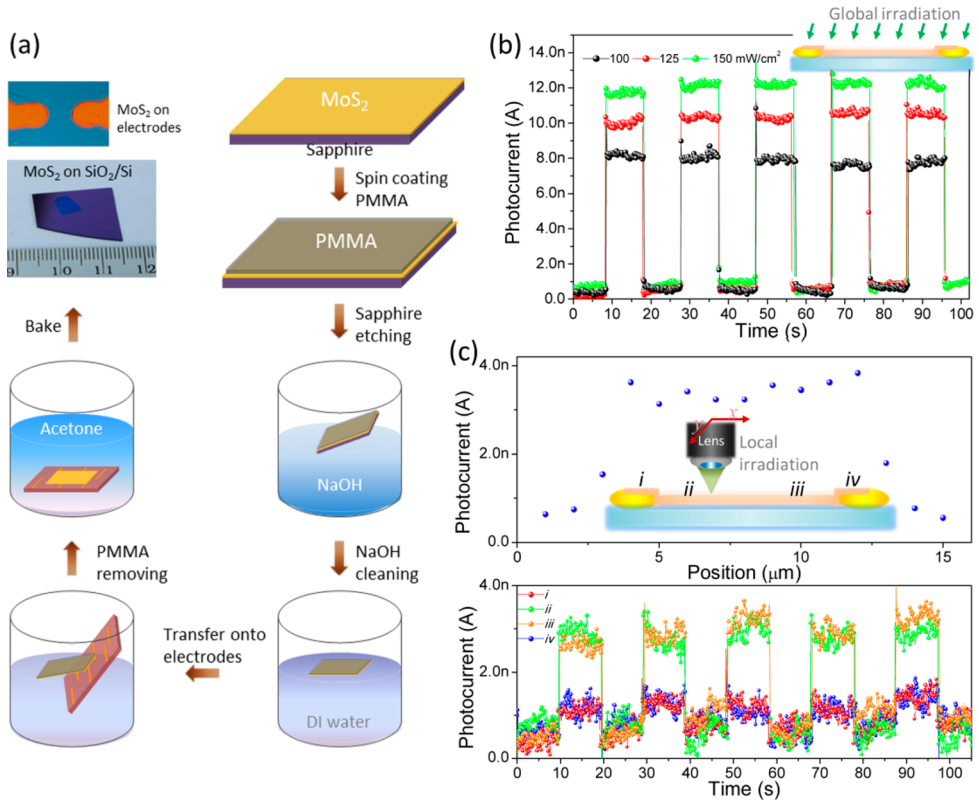

Figure 3. (a) Schematic of MoS_2 film transfer and device assembly processes. Photoresponse characteristics of pristine device under (b) broad beam and (c) focused laser beam irradiation.

film (few-layer thick). The gap between the electrodes is 10 μm wide. Optoelectronics is a significant potential application expected in TMDCs.[5] To demonstrate this attribute, the fabricated device was studied as a photodetector. A beam of laser light (λ = 532 nm) was globally and periodically irradiated on the whole device at a bias of 3 V, as shown by the schematic in Figure 3b. The photoresponse characteristics of the device under the influence of laser light at different laser powers are shown in Figure 3b. In this experiment, we ensured that the laser powers were much lower than that used for laser thinning experiment. The laser beam was illuminated onto the sample periodically. The output of the device presented a corresponding rapid on and off behavior with an on/off current ratio of about 20 under 100 mW/cm^2. The photoresponsivity was calculated to be around 0.12 A/W according to the formula $R = (I_{illum} - I_{dark})S^{-1}/P_{inc}$, where I_{illum} and I_{dark} are the output current under illuminated and in dark conditions, respectively. S is the effective working area (defined by the area between two electrodes) of the device. P_{inc} is power density of the incident light. The rapid photoresponse and reasonably high responsivity indicate a better performance than monolayer MoS_2 photodetectors[24] and phototransistors,[25] while comparable to the reported few-layer MoS_2 photodetector.[26] Notably, our focused laser beam system could be utilized as a home-built scanning photocurrent microscope (SPCM). Namely, by focusing the laser spot onto selected position on the MoS_2 film between the two electrodes, we could pinpoint the photoresponse of the device upon targeted laser irradiation at the selected positions. Figure 3c, inset schematically illustrates the measurement process where a focused microsize laser spot was scanned along the device. The line scan under applied bias of 3 V is shown in the upper panel of Figure 3c. Evidently, the profile is almost flat whenever the focused laser beam was irradiated on the MoS_2 film. This indicates the photocurrent did not show obvious difference along the device. The photoresponse behavior at selective positions was also recorded as shown in bottom panel of Figure 3c. In work area *ii* and *iii*, the output showed almost the same rapid on and off behavior with similar responsivity. This indicates the spatially uniform photoresponse of the photodetector.

To extend the usefulness of the focused laser beam setup, patterned MoS_2 film with monolayer–multilayer junctions was fabricated and investigated as high performance optoelectronic device. Starting with device with few-layer MoS_2 film, we used the focused laser beam to modify part of the MoS_2 film that bridged across the two electrodes. As shown in the inset in Figure 4a, we used the laser thinning method to define a microbox of about 30 μm $\times$ 30 μm such that the left edge of the box resided in between the two electrodes. Thus, in the event of the flow of electrical current, the current would flow across a junction with few-layer and

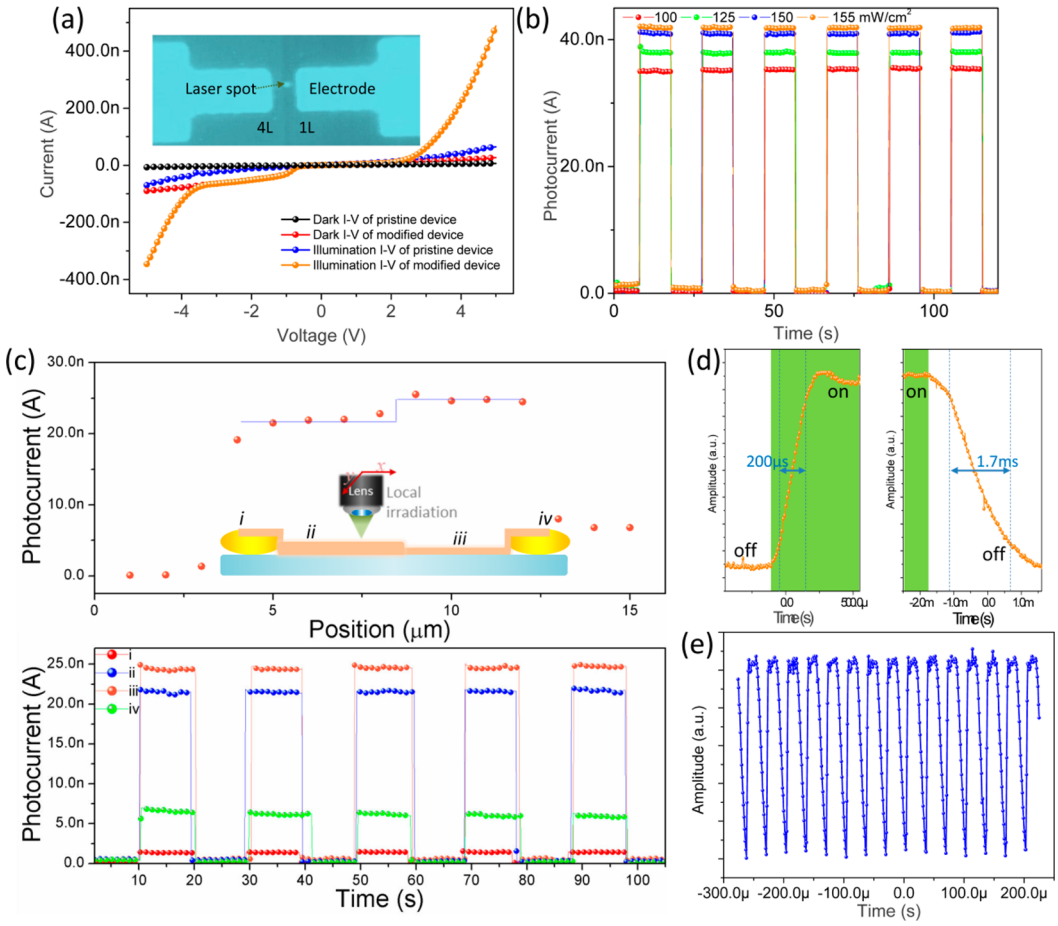

Figure 4. (a) Typical *I*−*V* characteristics of pristine and modified devices at dark and laser illumination condition. Photoresponse characteristics of laser modified device under (b) broad beam and (c) focused laser beam irradiation. (d) Photocurrent rising and delay rate test of the device. (e) Fast photoswitching behavior demonstration.

monolayer MoS_2. We did this progressively in such a way that the few-monolayer junction was located at a distance of 2.5, 5 (*i.e.*, half way), and 7.5 μm from the electrode on the right. For completeness, eventually all the MoS_2 between the two electrodes are thinned down.

The typical *I*−*V* characteristics of pristine device and laser modified device where the few-monolayer junction was located at midway between the electrodes are shown in Figure 4a. Evidently, the output curve changed from symmetrical form to asymmetrical form after laser modification, while the output current increased. A possible explanation is due to the increasing defect concentration caused by the focused laser modification. As predicted by Zhou *et al.*, the concentration of various defects can be deliberately induced *via* irradiation by high energy particles or high energy laser.[27] Notably a step appears at $V \sim -0.7$ V. This was probably attributed to the built-in potential barrier in the created monolayer−multilayer junction. The output of both devices obviously increased upon laser light illumination as revealed by the blue and orange *I*−*V* curves in Figure 4a. Due to the enabled band gap engineering and existence of the built-in potential barrier, better photodetection performance was expected for the laser-modified device. Similar to the device with pristine MoS_2 film, the device was subjected to global and periodic illumination of laser beam (λ = 532 nm) at different laser powers. During the experiment, the bias across the electrode was maintained at 3 V, while we monitored the electric current that flows across the electrodes. The results are shown in Figure 4b. As compared with the pristine device, the photocurrent value increased around 4−5 times at the same incident laser power (100 mW/cm^2). The corresponding responsivity could be calculated to be around 0.55 A/W. The enhanced photoresponse performance could be attributed to the built-in different functional domains created within MoS_2 films. In addition, the laser modification approach would introduce defects into the materials, which could result in increasing conductivity and photoconductivity.[28] To investigate the influence of laser modification to photoresponse, SPCM was employed to measure the localized photocurrent by scanning the focused laser beam along a line across the electrodes. Remarkably, the laser modified region (monolayer) presented higher photocurrent values than those presented by pristine region (multilayer)

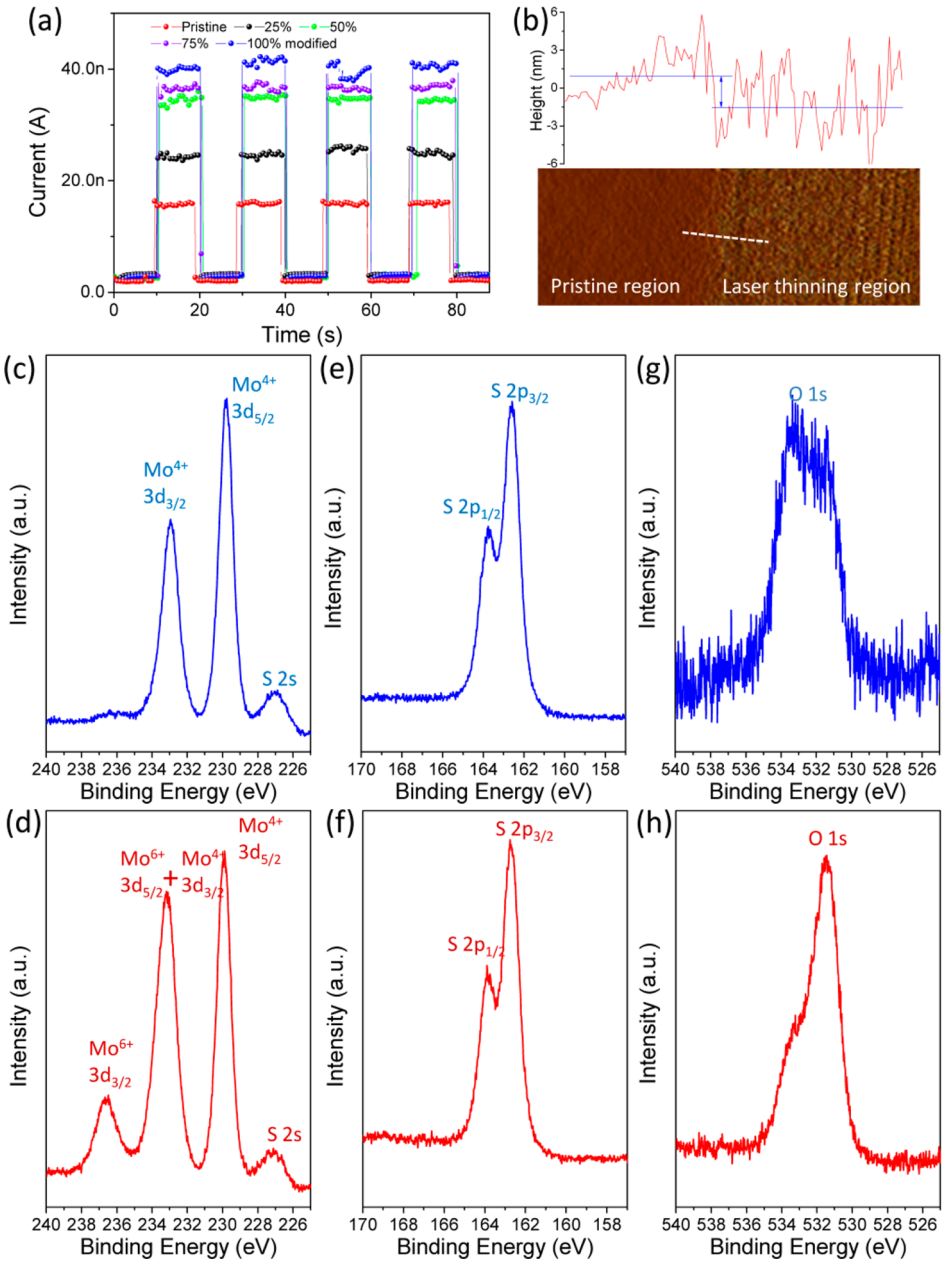

Figure 5. (a) Photoresponse characteristics of devices with different laser modified areas. (b) AFM image and the height profile of the device cross the junction between the pristine and laser pruning regions. XPS scans for Mo (c) before and (d) after laser modification. XPS scans for S (e) before and (f) after laser modification. XPS scans for O (g) before and (h) after laser modification.

as shown in the upper panel of Figure 4c. The on and off behavior of four selected positions were measured and shown in bottom panel of Figure 4c. Evidently, the position *iii* within modified region showed higher photocurrent value than that of position *ii* within pristine region. This result indicated the focused laser beam patterning was an effective approach to promote the functionality of 2D MoS_2 optoelectronic device. The fast photoresponse time of the modified device was estimated from the photocurrent *versus* time plots under a monitor of oscilloscope and shown in Figure 4d. The schematic diagram of the measurement setup is shown in Figure S3. The rise time is defined as the time needed to reach 90% of the photocurrent from dark current value upon laser irradiation and the decay time is defined as the time needed for the current value to drop to 10% after the light was switched off. Accordingly, 0.2 ms of the rise and 1.7 ms of the decay times could be obtained from the oscilloscope. These rapid response times are much faster than most of the reported organic and inorganic photodetectors/sensors.[29−33] The photoswitching frequency could be further improved as fast as 3.3 kHz (Figure 4e), which was limited by the sensitivity of our equipment. The photoswitching behaviors of the device at different frequency were shown in Figure S4.

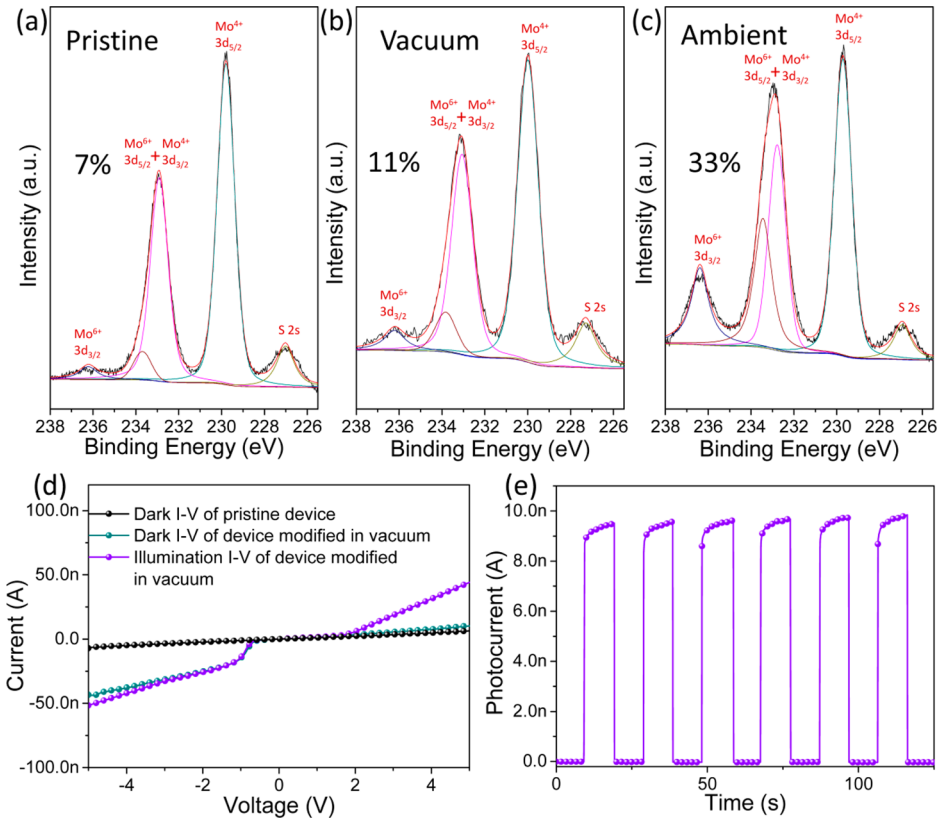

Figure 6. XPS scans for Mo of (a) pristine sample, samples modified in (b) vacuum, and modified in (c) ambient. (d) Typical output characteristics of pristine and modified in vacuum devices. (e) Photoresponse characteristics of device that laser modified in vacuum.

Systematic experiments have been carried out to investigate the influence of laser modified area to photoresponse. Initially, a device, where a quarter of film materials between the two electrodes was thinned down, was measured and the photoresponse characteristic was shown in Figure 5a. The photocurrent obviously increased as compared with pristine device. Subsequently, the proportion of the film materials thinned down by the focused laser beam was increased gradually to half of the working area, three-quarters of the working area and finally the entire working area was modified by laser thinning. The corresponding photoresponse characteristics were measured and shown in Figure 5a. Evidently, the photocurrent values increased with increased proportion of modified area. This is suggestive of the possibility that the surface photoelectrical property of MoS_2 films was improved by the laser modification. The surface modification of the device was investigated by AFM and XPS. The junction of the pristine and laser thinned regions of the device was scanned by AFM and the image is shown in Figure 5b. Evidently, the thickness of the films decreased by about three layers as revealed by the height profile. However, the roughness of the laser thinned region became about 3−4 times larger than that of the pristine region. The detailed surface chemical modification was probed further by XPS. Figure 5c−h displays detailed XPS scans for the Mo, S, and O binding energies of the film before and after laser modification. For the pristine region, the Mo 3d shows two peaks at 229.5 and 232.8 eV (Figure 5c), attributed to the doublet Mo $3d_{5/2}$ and Mo $3d_{3/2}$, respectively. The peaks located at 163.8 and 162.3 eV (Figure 5e) are assigned to be the S $2p_{1/2}$ and S $2p_{3/2}$ orbital of divalent sulfide ions (S^{2-}). The small O 1s peak around 533 eV (Figure 5g) is probably resulted from the SiO_2 substrate. All these results are consistent with reported MoS_2 thin films and crystals.[20,34] After laser modification (Figure 5d), beside the two Mo^{4+} peaks, an additional small peak located at 236.3 eV is observed which is attributed to the $3d_{3/2}$ binding energy for Mo^{6+}. The original peak at 232.8 eV becomes higher and broader. This is due to the coexisting of Mo^{6+} $3d_{5/2}$ and Mo^{4+} $3d_{3/2}$.[15,35] The peaks of S 2p (Figure 5f) do not show significant changes after laser modification while an additional peak at 531.2 eV is observed (Figure 5h). This peak is consistent with the reported O 1s peak in MoO_3.[35] Therefore, these results indicate that the focused laser beam modification could easily give rise to the surface oxidation or introduce oxygen doping into the MoS_2 films. On the basis of this surface morphology and surface chemical modification, the photoelectrical properties of the films could be properly promoted. To verify this

possible mechanism, we carried out the laser modification of the sample with the sample housed in a vacuum chamber (see Figure 2a). In doing so, the oxidization effect would be effectively reduced. The laser power was controlled at around 85 mW after focused by the objective lens and the scan speed was maintained at around 50 μm/s during the modification process. The Mo XPS scans of pristine film and films modified at vacuum and ambient conditions are shown in Figure 6a–c. The peaks are identified and fitted by Gaussian curves. After fitting, the MoO_3 ratios (identified as $(Mo^{6+}/(Mo^{6+} + Mo^{4+}))$) are calculated to be around 7%, 11%, and 33%, respectively. This indicates that modification in vacuum would not significantly result in the surface oxidation or introduce oxygen doping into the MoS_2 films. The photodetector device is fabricated based on the films modified in vacuum. The corresponding typical $I-V$ output in dark condition and under illumination and the photoresponse characterization are shown in Figure 6d,e. Evidently, the photocurrent of the corresponding device is measured to be lower than 10 nA at 100 mW/cm^2 illumination. This value is comparable with pristine device but much less than the device modified in ambient (Figure 4b). These results indicate that the laser modification induced surface oxygen doping plays the dominant role in improving the photoelectrical property of MoS_2 films.

CONCLUSION

In conclusion, we have demonstrated an inherently efficient and high throughput technique to directly pattern large area MoS_2 films. Well-defined micro structures are achievable *via* a simple focused laser beam. Remarkably, the thickness of the created patterns can be precisely controlled with this effective technique. As a result, different band gap domains at the same film can be facilitated due to the layer-dependent band gap engineering in MoS_2. In addition, the surface property of the modified region is altered by the laser modification. Therefore, the formed junctions and modified patterns will functionalize the 2D MoS_2 films. On the basis of this, a superior photodetector was fabricated and demonstrated.

METHODS

Preparation of MoS_2 Films. Large area MoS_2 monolayer and few-layer films were synthesized by a self-limiting growth approach.[17] A schematic diagram of the growth reactor is shown in Figure 1a. Typically, 0.5–5 mg of $MoCl_5$ powder was loaded in a ceramic boat and inserted into the center of a horizontal tube furnace. Then, 1 g of sulfur powder was placed at the upstream of the furnace. Different types of substrates (sapphire, quartz or Si with 300 nm SiO_2) were placed beside the $MoCl_5$ source. During the growth, the furnace was ramped to 900 °C at the rate of 40 °C/min. The sulfur powder was heated separately to 200 °C, and the vapor was carried by He gas to the center at a constant flow rate of 20 sccm with the pressure regulated and maintained at 1 Torr. The furnace was maintained at 900 °C for 15 min before cooling to room temperature naturally. The thickness of the MoS_2 films was controlled by adjusting the amount of precursor. After synthesis, postannealing in sulfur ambient was carried out to improve the crystalline quality.[20]

Characterization of MoS_2 Films. The as-grown and laser pruned samples were characterized by optical microscopy (Olympus BX51), Atomic Force Microscope AFM (Veeco D3000), X-ray Photoelectron Spectroscopy XPS, micro-Raman and photoluminescence spectroscopy (Renishaw inVia 2000, 532 nm).

Device Fabrication and Measurement. First, the source-drain electrodes (8/30 nm Cr/Au) were patterned and deposited on the substrate (300 nm SiO_2/Si) by photolithography and electron beam deposition. Subsequently, the as-grown MoS_2 films were transferred onto the substrate to cover the electrodes by a standard transfer approach. To obtain a better contact, thermal annealing was performed in Ar atmosphere at 200 °C for 15 min. Two approaches were implemented for photodetector device measurement: a globally illumination approach where the laser was directly irradiated as a broad beam on the whole device, and a local illumination approach where the laser beam was focused on selected positions of the device with a laser spot size of 1–2 μm.

Conflict of Interest: The authors declare no competing financial interest.

Acknowledgment. The authors gratefully acknowledge the financial support from Singapore National Research Foundation under CRP Award No. NRF-CRP-4-2008-03.

Supporting Information Available: Optical images of large area MoS_2 films with different layer numbers on different substrates, extended PL spectrum, schematic of fast photoresponsse rate measurement, and photoswitching behavior of the photodetectors. This material is available free of charge *via* the Internet at http://pubs.acs.org.

REFERENCES AND NOTES

1. Geim, A. K.; Novoselov, K. S. The Rise of Graphene. *Nat. Mater.* **2007**, *6*, 183–191.
2. Castro Neto, A. H.; Guinea, F.; Peres, N. M. R.; Novoselov, K. S.; Geim, A. K. The Electronic Properties of Graphene. *Rev. Mod. Phys.* **2009**, *81*, 109–162.
3. Radisavljevic, B.; Radenovic, A.; Brivio, J.; Giacometti, V.; Kis, A. Single-Layer MoS_2 Transistors. *Nat. Nanotechnol.* **2011**, *6*, 147–150.
4. Mak, K. F.; Lee, C.; Hone, J.; Shan, J.; Heinz, T. F. Atomically Thin MoS_2: A New Direct-Gap Semiconductor. *Phys. Rev. Lett.* **2010**, *105*, 136805.
5. Wang, Q. H.; Kalantar-Zadeh, K.; Kis, A.; Coleman, J. N.; Strano, M. S. Electronics and Optoelectronics of Two-Dimensional Transition Metal Dichalcogenides. *Nat. Nanotechnol.* **2012**, *7*, 699–712.
6. Kuc, A.; Zibouche, N.; Heine, T. Influence of Quantum Confinement on the Electronic Structure of the Transition Metal Sulfide TS_2. *Phys. Rev. B* **2011**, *83*, 245213.
7. Splendiani, A.; Sun, L.; Zhang, Y.; Li, T.; Kim, J.; Chim, C.-Y.; Galli, G.; Wang, F. Emerging Photoluminescence in Monolayer MoS_2. *Nano Lett.* **2010**, *10*, 1271–1275.
8. Zhan, Y.; Liu, Z.; Najmaei, S.; Ajayan, P. M.; Lou, J. Large-Area Vapor-Phase Growth and Characterization of MoS_2 Atomic Layers on a SiO_2 Substrate. *Small* **2012**, *8*, 966–971.
9. Lee, C.; Yan, H.; Brus, L. E.; Heinz, T. F.; Hone, J.; Ryu, S. Anomalous Lattice Vibrations of Single- and Few-Layer MoS_2. *ACS Nano* **2010**, *4*, 2695–2700.
10. Kim, S.; Konar, A.; Hwang, W.-S.; Lee, J. H.; Lee, J.; Yang, J.; Jung, C.; Kim, H.; Yoo, J.-B.; Choi, J.-Y.; Jin, Y. W.; Lee, S. Y.; Jena, D.; Choi, W.; Kim, K. High-Mobility and Low-Power Thin-Film Transistors Based on Multilayer MoS_2 Crystals. *Nat. Commun.* **2012**, *3*, 1011.

11. Zeng, H.; Dai, J.; Yao, W.; Xiao, D.; Cui, X. Valley Polarization in MoS_2 Monolayers by Optical Pumping. *Nat. Nanotecgnol.* **2012**, *7*, 490–493.
12. Lee, Y.-H.; Zhang, X.-Q.; Zhang, W.; Chang, M.-T.; Lin, C.-T.; Chang, K.-D.; Yu, Y.-C.; Wang, J. T.-W.; Chang, C.-S.; Li, L.-J.; Lin, T.-W. Synthesis of Large-Area MoS_2 Atomic Layers with Chemical Vapor Deposition. *Adv. Mater.* **2012**, *24*, 2320–2325.
13. van der Zande, A. M.; Huang, P. Y.; Chenet, D. A.; Berkelbach, T. C.; You, Y.; Lee, G.-H.; Heinz, T. F.; Reichman, D. R.; Muller, D. A.; Hone, J. C. Grains and Grain Boundaries in Highly Crystalline Monolayer Molybdenum Disulphide. *Nat. Mater.* **2013**, *12*, 554–561.
14. Najmaei, S.; Liu, Z.; Zhou, W.; Zou, X.; Shi, G.; Lei, S.; Yakobson, B. I.; Idrobo, J.-C.; Ajayan, P. M.; Lou, J. Vapour Phase Growth and Grain Boundary Structure of Molybdenum Disulphide Atomic Layers. *Nat. Mater.* **2013**, *12*, 754–759.
15. Lin, Y.-C.; Zhang, W.; Huang, J.-K.; Liu, K.-K.; Lee, Y.-H.; Liang, C.-T.; Chu, C.-W.; Li, L.-J. Wafer-Scale MoS_2 Thin Layers Prepared by MoO_3 Sulfurization. *Nanoscale* **2012**, *4*, 6637–6641.
16. Shi, Y.; Zhou, W.; Lu, A.-Y.; Fang, W.; Lee, Y.-H.; Hsu, A. L.; Kim, S. M.; Kim, K. K.; Yang, H. Y.; Li, L.-J.; Idrobo, J.-C.; Kong, J. van der Waals Epitaxy of MoS_2 Layers Using Graphene As Growth Templates. *Nano Lett.* **2012**, *12*, 2784–2791.
17. Yifei, Y.; Chun, L.; Yi, L.; Liqin, S.; Yong, Z.; Linyou, C., Controlled Scalable Synthesis of Uniform, High-Quality Monolayer and Few-layer MoS_2 Films. *Sci. Rep.* **2013**, *3*.
18. Liu, Y.; Nan, H.; Wu, X.; Pan, W.; Wang, W.; Bai, J.; Zhao, W.; Sun, L.; Wang, X.; Ni, Z. Layer-by-Layer Thinning of MoS_2 by Plasma. *ACS Nano* **2013**, *7*, 4202–4209.
19. Castellanos-Gomez, A.; Barkelid, M.; Goossens, A. M.; Calado, V. E.; van der Zant, H. S. J.; Steele, G. A. Laser-Thinning of MoS_2: On Demand Generation of a Single-Layer Semiconductor. *Nano Lett.* **2012**, *12*, 3187–3192.
20. Liu, K.-K.; Zhang, W.; Lee, Y.-H.; Lin, Y.-C.; Chang, M.-T.; Su, C.-Y.; Chang, C.-S.; Li, H.; Shi, Y.; Zhang, H.; Lai, C.-S.; Li, L.-J. Growth of Large-Area and Highly Crystalline MoS_2 Thin Layers on Insulating Substrates. *Nano Lett.* **2012**, *12*, 1538–1544.
21. Li, H.; Zhang, Q.; Yap, C. C. R.; Tay, B. K.; Edwin, T. H. T.; Olivier, A.; Baillargeat, D. From Bulk to Monolayer MoS_2: Evolution of Raman Scattering. *Adv. Funct. Mater.* **2012**, *22*, 1385–1390.
22. Eda, G.; Yamaguchi, H.; Voiry, D.; Fujita, T.; Chen, M.; Chhowalla, M. Photoluminescence from Chemically Exfoliated MoS_2. *Nano Lett.* **2011**, *11*, 5111–5116.
23. Kuc, A.; Zibouche, N.; Heine, T. Influence of Quantum Confinement on the Electronic Structure of the Transition Metal Sulfide TS_2. *Phys. Rev. B* **2011**, *83*, 245213.
24. Zhang, W.; Huang, J.-K.; Chen, C.-H.; Chang, Y.-H.; Cheng, Y.-J.; Li, L.-J. High-Gain Phototransistors Based on a CVD MoS_2 Monolayer. *Adv. Mater.* **2013**, *25*, 3456–3461.
25. Yin, Z.; Li, H.; Li, H.; Jiang, L.; Shi, Y.; Sun, Y.; Lu, G.; Zhang, Q.; Chen, X.; Zhang, H. Single-Layer MoS_2 Phototransistors. *ACS Nano* **2011**, *6*, 74–80.
26. Tsai, D.-S.; Liu, K.-K.; Lien, D.-H.; Tsai, M.-L.; Kang, C.-F.; Lin, C.-A.; Li, L.-J.; He, J.-H. Few-Layer MoS_2 with High Broadband Photogain and Fast Optical Switching for Use in Harsh Environments. *ACS Nano* **2013**, *7*, 3905–3911.
27. Zhou, W.; Zou, X.; Najmaei, S.; Liu, Z.; Shi, Y.; Kong, J.; Lou, J.; Ajayan, P. M.; Yakobson, B. I.; Idrobo, J.-C. Intrinsic Structural Defects in Monolayer Molybdenum Disulfide. *Nano Lett.* **2013**, *13*, 2615–2622.
28. Lu, J.; Lim, X.; Zheng, M.; Mhaisalkar, S. G.; Sow, C.-H. Direct Laser Pruning of CdS_xSe_{1-x} Nanobelts en Route to a Multicolored Pattern with Controlled Functionalities. *ACS Nano* **2012**, *6*, 8298–8307.
29. Tang, Q.; Li, L.; Song, Y.; Liu, Y.; Li, H.; Xu, W.; Liu, Y.; Hu, W.; Zhu, D. Photoswitches and Phototransistors from Organic Single-Crystalline Sub-micro/nanometer Ribbons. *Adv. Mater.* **2007**, *19*, 2624–2628.
30. Dong, H.; Li, H.; Wang, E.; Nakashima, H.; Torimitsu, K.; Hu, W. Phototransistors of a Rigid Rod Conjugated Polymer. *J. Phys. Chem. C* **2008**, *112*, 19690–19693.
31. Weng, W. Y.; Chang, S. J.; Hsu, C. L.; Hsueh, T. J. A ZnO-Nanowire Phototransistor Prepared on Glass Substrates. *ACS Appl. Mater. Interfaces* **2011**, *3*, 162–166.
32. Lu, J.; Sun, C.; Zheng, M.; Wang, Y.; Nripan, M.; van Kan, J. A.; Mhaisalkar, S. G.; Sow, C. H. Ultrasensitive Phototransistor Based on K-Enriched MoO_3 Single Nanowires. *J. Phys. Chem. C* **2012**, *116*, 22015–22020.
33. Hsu, C.-Y.; Lien, D.-H.; Lu, S.-Y.; Chen, C.-Y.; Kang, C.-F.; Chueh, Y.-L.; Hsu, W.-K.; He, J.-H. Supersensitive, Ultrafast, and Broad-Band Light-Harvesting Scheme Employing Carbon Nanotube/TiO_2 Core−Shell Nanowire Geometry. *ACS Nano* **2012**, *6*, 6687–6692.
34. Altavilla, C.; Sarno, M.; Ciambelli, P. A Novel Wet Chemistry Approach for the Synthesis of Hybrid 2D Free-Floating Single or Multilayer Nanosheets of MS2@oleylamine (M = Mo, W). *Chem. Mater.* **2011**, *23*, 3879–3885.
35. Torres, J.; Alfonso, J. E.; López-Carreño, L. D. XPS and X-ray Diffraction Characterization of MoO_3 Thin Films Prepared by Laser Evaporation. *Phys. Status Solidi C* **2005**, *2*, 3726–3729.